JOURNAL OF COMPUTATIONAL PHYSICS 26, 197–217 (1978)

The Calculation of Turbulent Recirculating Flows in General Orthogonal Coordinates

S. B. POPE[1]

Imperial College of Science and Technology, Department of Mechanical Engineering, Exhibition Road, London SW7 2BX

Received January 6, 1977; revised March 30, 1977

Many flows of practical interest, such as those that are bounded by curved surfaces, could be calculated in curvilinear coordinates more accurately, conveniently, and economically than in Cartesian coordinates. A calculation procedure is developed by representing the conservation equations in general orthogonal coordinates and so obtaining appropriate finite-difference equations. These equations are written in a similar manner to their Cartesian counterparts, thus enabling the procedure of Gosman and Pun (Imperial College Report HTS/73/2) to be adapted. The viability of such a procedure depends upon the ability to generate an orthogonal grid appropriate to a given flow geometry and consequently a grid-generation procedure is also developed: it is based on the solution, by an iterative finite-difference technique, of Laplace's equation for the Cartesian coordinates of the orthogonal grid nodes. The combined procedures are tested and demonstrated by calculating the flow properties in a diffuser of sufficient divergence to cause recirculation.

1. INTRODUCTION

Several recent papers, [1–4], for example, have reported solutions of partial differential equations appropriate to recirculating flows. These equations were expressed in Cartesian or polar–cylindrical coordinates, rewritten in finite-difference form, and solved by an appropriate algorithm. In general, the geometric configuration of each flow situation was simple and the coordinate system used was a natural choice in that the flow boundaries were coincident with coordinate lines. Consequently, the finite-difference solution domain lay entirely within the flow field and, close to boundaries, the grid could be selectively refined in order to retain numerical accuracy in regions of high gradients: also, the coincidence of the boundaries with coordinate lines greatly simplified the specification of boundary conditions.

There are, however, a variety of flows of practical interest for which rectangular coordinates are less appropriate and the previously mentioned benefits are lost. Separated flow in the vicinity of curved surfaces such as airfoils and turbine blades is better represented in a coordinate system which follows the curvature and so allows skin friction and heat transfer to be computed accurately. Similarly, a nonrectangular

[1] Present address: California Institute of Technology, Department of Applied Mathematics, Pasadena, California 91125.

0021-9991/78/0262-0197$02.00/0

coordinate system is more suited to the calculation of the flow in gas-turbine combustion chambers of varying radius. A further example is provided by the separated flow in the curved diffuser sketched in Fig. 1. Figures 1a and 1b show this flow in rectangular and nonrectangular coordinates, respectively, and the advantages of the latter are apparent: the grid can be refined in the two boundary layers, the boundary conditions can be easily and more accurately imposed, and no wastage is caused by grid nodes external to the flow.

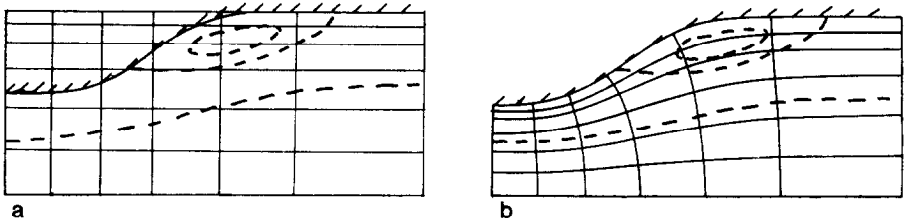

FIG. 1. Sketch of flow in a diffuser: (a) rectangular coordinates; (b) curvilinear coordinates.

Numerical methods have been developed to solve the conservation equations governing the flow in general curvilinear coordinates [5, 6] but the complicated form adopted by the equations in these coordinates entails additional expense in terms of computer resources. However, in many situations an orthogonal grid is equally effective and the equations in orthogonal form are little more complicated than their Cartesian counterparts. One purpose of the present report is, therefore, to represent the elliptic equations, appropriate to viscous recirculating flow, in general orthogonal coordinates and to deduce the corresponding finite-difference equations. A novel procedure, developed for transforming equations into general orthogonal coordinates, has been used to obtain the transport equations for velocity and a general scalar quantity which may represent turbulent, thermodynamic, or chemical properties of the flow. Appropriate turbulence equations are discussed by Launder and Spalding [7] and by Pope and Whitelaw [2] and equations to characterize turbulent reaction are appraised by Pope [8]. The finite-difference equations are presented for two-dimensional flows although the procedure is quite general.

It will be shown that the equations can be solved as easily in orthogonal coordinates as in rectangular coordinates but an orthogonal grid, appropriate to a given flow geometry, cannot be specified as simply as a rectangular mesh. A second purpose of the report is, therefore, to describe a method for generating an orthogonal grid which is essential to the procedure as a whole. Barfield [9] developed a mapping procedure to generate orthogonal grids but, for consistency with the main exercise, it was decided to develop a finite-difference method. Amsden and Hirst [10] and Thompson *et al.* [11] reported finite-difference grid-generation procedures but they are not intended to produce orthogonal grids. The procedure reported here solves Laplace's equation for the Cartesian coordinates of the orthogonal grid nodes by an iterative finite-difference technique and the only obstacle that was overcome in its

development was the determination and application of the appropriate boundary conditions.

The solution method used to generate the grid nodes is also able to provide solutions to the potential-flow equations in a particularly convenient way. This is because the location of the streamlines can be made the subject of the equations (solved in stream-function space) rather than the normal practice of solving for stream function in position space: thus rather than specifying a constant value of stream function over the perimeter of a body or along a streamline, the coordinates of the body or streamline are specified for a constant value of the stream function. As a consequence, for unconfined flows, the procedure is able to generate free-stream boundary conditions for the velocity components which are necessary to the solution of the elliptic equations. Thus, the matching of the potential flow with the viscous flow procedure is achieved in an efficient manner.

The contributions mentioned above are described in the next four sections entitled, "Transport Equations," "Equations in Orthogonal Coordinates," "Finite-Difference Method," and "Grid-Generation Procedure." In the final section, results of calculations designed to test the procedure are presented and discussed.

2. Transport Equations

In this section the differential equations which represent the flow are presented and discussed. The presentation of the equations in customary Cartesian tensor notation is intended to convey the physical basis of the equations without introducing complicated or unfamiliar notation appropriate to more general coordinate systems.

The continuity and momentum equations for a flow without body forces are:

$$(\partial\rho/\partial t) + (\partial\rho U_i/\partial x_i) = 0 \tag{1}$$

and

$$(\partial\rho U_j/\partial t) + (\partial\rho U_i U_j/\partial x_i) = -(\partial p/\partial x_j) - (\partial\tau_{ij}/\partial x_i) \tag{2}$$

where $\rho(\mathbf{x}, t)$ is the averaged density at position $\mathbf{x}$ and time t: $\mathbf{U}$ is the averaged velocity, p the pressure, and τ_{ij} the stress tensor. The unknown Reynolds stresses, which at the high Reynolds number considered here are the only contributors to τ_{ij}, are determined from the $k - \epsilon$ turbulence model in conjunction with the isotropic viscosity hypothesis,

$$\frac{\partial\rho k}{\partial t} + \frac{\partial\rho U_i k}{\partial x_i} = \frac{\partial}{\partial x_i}\frac{\mu_{\text{eff}}}{\sigma_k}\frac{\partial k}{\partial x_i} + P - \rho\epsilon, \tag{3}$$

$$\frac{\partial\rho\epsilon}{\partial t} + \frac{\partial\rho U_i\epsilon}{\partial x_i} = \frac{\partial}{\partial x_i}\frac{\mu_{\text{eff}}}{\sigma_\epsilon}\frac{\partial\epsilon}{\partial x_i} + \frac{\epsilon}{k}(C_{\epsilon 1}P - C_{\epsilon 2}\rho\epsilon), \tag{4}$$

and

$$\tau_{ij} = -\mu_{\text{eff}}\left(\frac{\partial U_i}{\partial x_j} + \frac{\partial U_j}{\partial x_i}\right) + \frac{2}{3}\left(\rho k + \mu_{\text{eff}}\frac{\partial U_l}{\partial x_l}\right)\delta_{ij}. \tag{5}$$

Equations (3) and (4) account for the transport of the turbulent kinetic energy, k, and its rate of dissipation, ϵ. The production of kinetic energy and the effective viscosity are given by,

$$P = -(\partial U_i/\partial x_j)\,\tau_{ij} \tag{6}$$

and

$$\mu_{\text{eff}} = C_\mu \rho k^2/\epsilon \tag{7}$$

and the constants C_μ, $C_{\epsilon 1}$, $C_{\epsilon 2}$, σ_k, and σ_ϵ are ascribed the values 0.09, 1.45, 1.90, 1.0, and 1.3, respectively.

In addition to the hydrodynamic and turbulence equations, the transport equation for a general scalar quantity such as temperature or a mass fraction is also considered, i.e.,

$$\frac{\partial \rho \phi}{\partial t} + \frac{\partial \rho U_i \phi}{\partial x_i} = \frac{\partial}{\partial x_i}\frac{\mu_{\text{eff}}}{\sigma_\phi}\frac{\partial \phi}{\partial x_i} + S_\phi \tag{8}$$

where ϕ, the mass averaged value of the scalar, can also represent k and ϵ.

The closure provided by these equations was first used by Jones [12] although it stems from the earlier works of Chou [13] and Harlow and Nakayama [14]. A description of the modeling of the turbulence equation is given by Launder and Spalding [7] and for a criticism of the effective viscosity hypothesis and dissipation equation (which contain the major assumptions), the reader is referred to previous work [15, 16]. The only aspect of the modeling which requires further explanation is the treatment of density fluctuations caused either by compressibility or by temperature or species gradients: the conventionally averaged equations for velocity and kinetic energy contain correlations between density and velocity fluctuations, which ential further modeling assumptions and produce extra terms for incorporation in a calculation procedure. On the other hand, the use of mass-weighted averaging results in equations which are similar to their constant density counterparts and as has been argued [17], the same modeling can be employed. Consequently, all of the dependent variables in Eqs. (1)–(4), except ρ and p, are mass averaged and it may be noted that the isotropic viscosity hypothesis (Eq. (5)) has been modified to ensure that the Reynolds-stress tensor contracts correctly even when the divergence of velocity is nonzero.

The closure provided by these equations is completed by the specification of boundary conditions over the whole perimeter of the solution domain. The imposition of boundary conditions is straightforward except in near-wall regions where the following functions are added to the equations in order to account for the influence of laminar effects and to preclude the need for fine grid calculations in that region:

$$\tau_{\text{W}} = (U_p/y_p)(\mu y_p{}^+/\ln(E y_p{}^+))$$

where

$$y_p{}^+ = \rho(k_p C_\mu^{1/2})^{1/2}\,(y_p/\mu), \qquad \epsilon_p = (C_\mu^{1/2} k_p)^{3/2}/\kappa y_p\,,$$

and

$$\int_0^{y_p} \epsilon dy = (C_\mu^{1/2} k_p)^{3/2}\,\frac{1}{\kappa}\ln(E y_p{}^+).$$

τ_w is the wall shear stress and μ the laminar viscosity. The subscript p refers to the grid node next to the wall and y_p and U_p are the normal distance and parallel velocity at that point. κ and E are the constants in the logarithmic law-of-the-wall and have values of 0.4 and 8.8.

3. Equations in Orthogonal Coordinates

In order to formulate finite-difference equations in general orthogonal coordinates, a less restricted representation of the equations presented above is required. The novel notation for orthogonal coordinates, introduced below, is well suited to this task in that it is a compromise between the simplicity of Cartesian tensor notation and the versatility of general tensors. There are a variety of ways in which the equations can be expressed in general orthogonal coordinates and many ways of performing the transformations: here, the equations are expressed in terms of the physical components of the tensors and the transformations are performed by a novel procedure. The justification for these choices is that the result is a simple and compact expression of the equations which retain their physical significance: the advantage of the compact notation is not merely aesthetic but leads to simple finite-difference equations and, consequently, to computational economy.

Figure 2 is a sketch of an orthogonal coordinate system (in two dimensions for simplicity) where the orthogonal coordinates x^i are shown relative to Cartesian coordinates $\bar{x}^i$. Distances in the general orthogonal coordinate system are relaetd to the Cartesian system through the metric tensor g_{ij} by

$$(ds)^2 = (d\bar{x}^i)^2 = g_{ij}\, dx^i\, dx^j \tag{9}$$

where

$$g_{ij} = \sum_l \frac{\partial \bar{x}^l}{\partial x^i} \frac{\partial \bar{x}^l}{\partial x^j} . \tag{10}$$

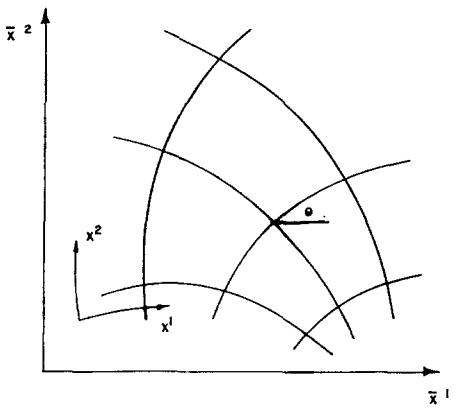

FIG. 2. Orthogonal coordinate lines in Cartesian coordinates, $\bar{x}$.

It follows from the definition of orthogonality that only the diagonal elements of the metric tensor are nonzero and so (9) can be written in the simple form

$$(ds)^2 = (d\bar{x}^i)^2 = (h_i\, dx^i)^2 = [dx(i)]^2 \tag{11}$$

where the scale factors h, which are excluded from the summation convention, are given by

$$h_i \equiv (g_{ii})^{1/2} \qquad \text{(no summation on } i\text{)}. \tag{12}$$

The physical components of displacement $dx(i)$, which are defined by (11), represent displacements along coordinate lines measured relative to the coordinate system $\bar{x}$. Similarly, the physical components of a contravariant vector are given by

$$A(i) \equiv h_i A^i \tag{13}$$

and represent the components of the vector in the direction of the coordinate lines measured relative to the Cartesian system. The advantages of expressing the transport equations in physical rather than co- or contra-variant form are that the vectors retain the same dimensions in all directions and all locations and that no additional terms arise due to stretching the coordinate system.

The transport equations in general orthogonal form could be derived from control volume analysis, obtained by intuition or from geometric transformations, but all of these methods are prone to error. On the other hand, the transformation of the equations into general tensor notation and subsequent simplification for orthogonal coordinates can, in principle, be performed with rigor, but the tedium of the algebra virtually ensures erroneous results. The novel procedure adopted here is to transform the equations in Cartesian form directly into the general orthogonal system by way of the transformations derived in Appendix I. These transformations are obtained rigorously by using general tensors and involve the derivative $\partial/\partial x(i)$, the divergence operator $\nabla(i)$, and coordinate variation terms $H_i(j)$ where,

$$\nabla(i) \equiv h_i \mid h \mid^{-1} \partial/\partial x(i) \mid h \mid/h_i \tag{14}$$

and

$$H_i(j) \equiv 1/h_i h_j\, \partial h_i/\partial x_j = \partial/\partial x(j) \ln h_i\,. \tag{15}$$

In Eq. (14), $\mid h \mid$ is the product of the scale factors and represents the volume ratio between the coordinate systems: the coordinate variation term, $H_i(j)$, represents the inverse of the radius of curvature of the j coordinate line and the suffix i is excluded from the summation convention. Quantities $\bar{A}$ in the Cartesian system $\bar{x}$ are transformed to quantities A in a general orthogonal system x by the following transformations:

Scalars.

$$\bar{A} \to A,$$
$$\partial\bar{A}/\partial\bar{x}_i \to \partial A/\partial x(i).$$

Vectors.

$$\bar{A}_i \to A(i),$$
$$\partial \bar{A}_i/\partial \bar{x}_j \to [\partial A(i)/\partial x(j)] - A(j)\, H_j(i) + A(k)\, H_i(k)\, \delta_{ij},$$
$$\partial \bar{A}_i/\partial \bar{x}_i \to \nabla(i)\, A(i).$$

Second-order tensors.

$$\bar{A}_{ij} \to A(ij),$$
$$\partial \bar{A}_{ij}/\partial \bar{x}_i \to \nabla(i)\, A(ij) - A(ii)\, H_i(j) + H_j(k)\, A(jk).$$

Appendix I contains general expressions for all transformations but those quoted above are sufficient to transform the transport equations as follows:

$$\partial \rho/\partial t + \nabla(i)[\rho U(i)] = 0, \tag{16}$$

$$\partial \rho U(j)/\partial t + \nabla(i)[\rho U(i)\, U(j) + \tau^*(ij)] = -\partial p^*/\partial x(j) + H_i(j)[\rho U(i)\, U(i) + \tau^*(ii)] - H_j(i)[\rho U(i)\, U(j) + \tau^*(ij)], \tag{17}$$

$$\partial \rho \phi/\partial t + \nabla(i)[\rho U(i)\phi - (\mu_{\text{eff}}/\sigma_\phi)\, \partial \phi/\partial x(i)] = S_\phi, \tag{18}$$

where the isotropic component of the turbulent stress has been added to the pressure, i.e.,

$$p^* = p + \tfrac{2}{3}\rho k + \tfrac{2}{3}\mu_{\text{eff}} \nabla(i)\, U(i) \tag{19}$$

and τ^* contains the anisotropic stresses,

$$\tau^*(ij) = -\mu_{\text{eff}} \left[\frac{\partial U(i)}{\partial x(j)} + \frac{\partial U(j)}{\partial x(i)} - U(i)\, H_i(j) - U(j)\, H_j(i) + 2U(l)\, H_i(l)\, \delta_{ij}\right]. \tag{20}$$

The production of turbulent kinetic energy is given by

$$\begin{aligned} P = {} & -\tau^*(ij)\left[\frac{\partial U(i)}{\partial x(j)} - U(j)\, H_j(i) + U(l)\, H_i(l)\, \delta_{ij}\right] \\ & - \frac{2}{3}[\rho k + \mu_{\text{eff}} \nabla(i)\, U(i)]\, \nabla(l)\, U(l) \\ = {} & \frac{1}{2}\mu_{\text{eff}} \left[\frac{\partial U(i)}{\partial x(j)} + \frac{\partial U(j)}{\partial x(i)} - U(i)\, H_i(j) - U(j)\, H_j(i) \right. \\ & \left. + U(l)\, \delta_{ij}[H_i(l) + H_j(l)]\right]^2 - \frac{2}{3}[\rho k + \mu_{\text{eff}} \nabla(i)\, U(i)]\, \nabla(l)\, U(l). \end{aligned} \tag{21}$$

The physical interpretation of the scalar transport equation is straightforward and not unexpected; the change of $\rho\phi$ in time is balanced by the inflow of ϕ due to convection and to gradient diffusion and by the source. The same form is adopted by the continuity equation but the momentum equation has gained source terms

due to coordinate curvature: these terms reflect the fact that momentum is conserved in a straight line not along a coordinate line. Thus, for example, the term

$$S(j) = H_i(j)\,\rho U(i)\,U(i) - H_j(i)\,\rho U(i)\,U(j) \tag{22}$$

represents a transfer of momentum for one coordinate direction to another and, since $S(j)\,U(j)$ is zero, the transfer is conservative. That is, $S(j)$ affects the direction of the velocity vector relative to the orthogonal coordinate system but not its length since the source due to $S(j)$ in the equation for $U(j)\,U(j)$ is zero. The additional terms in the relations for the stress tensor and the production of kinetic energy arise from the transformation of the velocity gradients and, as can be seen, P can be expressed as the sum of an identically nonnegative term due to the rate-of-strain and a term due to the divergence of velocity.

4. Finite-Difference Method

The calculation procedure solves the equations derived in the last section for steady, two-dimensional flows with,

$$U(1) = U, \qquad dx(1) = dx,$$
$$U(2) = V, \qquad dx(2) = dy.$$

In Appendix II, the differential equations for this situation are expanded and it is seen that they have the common form,

$$\nabla(1)(\rho U\psi - \Gamma_x\,\partial\psi/\partial x) + \nabla(2)(\rho V\psi - \Gamma_y\,\partial\psi/\partial y) = S_\psi \tag{23}$$

where the values of Γ_x, Γ_y, and S_ψ appropriate to each variable are given in Table I. The differences between this equation and its Cartesian counterpart lie solely in the divergence operator and the source terms and, consequently, it was possible to obtain a finite-difference procedure for orthogonal coordinates by modifying one for

TABLE I

ψ	Γ_x/μ_{eff}	Γ_y/μ_{eff}	S_ψ
1	0	0	0
U	2	1	$-\partial p^*/\partial x + 2\nabla_x[\mu_{eff} V H_1(2)] + H_1(2)[\mu_{eff}\,\partial U/\partial y - \rho UV]$ $+ [\nabla_y + H_1(2)]\{\mu_{eff}\,[\partial V/\partial x - VH_2(1) - UH_1(2)]\}$ $+ H_2(2)\{\rho V^2 - 2\mu_{eff}\,[\partial V/\partial y + UH_2(1)]\}$
k	$1/\sigma_k$	$1/\sigma_k$	$P - \rho\epsilon$
ϵ	$1/\sigma_\epsilon$	$1/\sigma_\epsilon$	$(\epsilon/k)(C_{\epsilon 1}P - C_{\epsilon 2}\rho\epsilon)$
ϕ	$1/\sigma_\phi$	$1/\sigma_\phi$	S_ϕ

Cartesian coordinates. Thus, the procedure reported here represents a modified version of that of Gosman and Pun [1] and details of the original procedure can be found in the above reference.

The finite-difference equations are obtained by integrating the equations over the (two-dimensional) volume indicated on the finite-difference grid, Fig. 3. The value

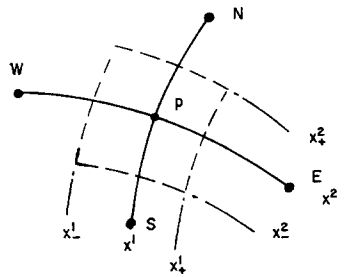

FIG. 3. Finite-difference cell.

of the variable ψ in question is assumed known at the nodes P, N, S, E, and W; P, N, and S and P, E, and W lie on lines of constant x^1 and x^2, respectively. The integration yields,

$$\left[\int_{x_-^2}^{x_+^2} \rho U\psi - \Gamma_x \frac{\partial \psi}{\partial x}\, dy\right]_{x_-^1}^{x_+^1} + \left[\int_{x_-^1}^{x_+^1} \rho V\psi - \Gamma_y \frac{\partial \psi}{\partial y}\, dx\right]_{x_-^2}^{x_+^2} = \int_{x_-^1}^{x_+^1}\int_{x_-^2}^{x_+^2} S_\psi\, dx\, dy. \quad (24)$$

The left-hand side of this equation is the area integral of the flux of ψ due for convection and diffusion which is balanced, on the right-hand side, by the volume integral of the source. The form of this equation is identical to its Cartesian counterpart although, it should be recalled, in this instance dx and dy are functions of the scale factors which, in turn, are functions of the coordinates. In general, the following finite-difference approximations are made:

$$\int_{x_-^2}^{x_+^2} \rho U\psi\, dy\,\Big|_{x_+^1} \approx \tfrac{1}{2}(\psi_P + \psi_E)(\rho U)_{x_+^1} \int_{x_-^2}^{x_+^2} dy = C_{x_+}(\psi_P + \psi_E), \quad (25)$$

$$\int_{x_-^2}^{x_+^2} \Gamma_x \frac{\partial \psi}{\partial x}\, dy\,\Big|_{x_+^1} \approx \left[(\psi_P - \psi_E)\Big/\int_{x_P^1}^{x_E^1} dx\right](\Gamma_x)_{x_+^1} \int_{x_-^2}^{x_+^2} dy = D_{x_+}(\psi_E - \psi_P), \quad (26)$$

and

$$\int_{x_-^2}^{x_+^2}\int_{x_-^1}^{x_+^1} S_\psi\, dx\, dy \approx (S_\psi)_P \int_{x_-^2}^{x_+^2}\int_{x_-^1}^{x_-^1} dx\, dy = (S_\psi)_P \text{ vol.} \quad (27)$$

Quantities such as $(\rho U)_{x_+^1}$ and $(\Gamma_x)_{x_+^1}$, if not known at the required locations, are obtained by interpolation and the remaining integrals are known functions of the grid.

Thus, a relation between ψ_P and neighboring values is obtained by substituting these approximations into Eq. (24),

$$\psi_P(A_N + A_S + A_E + A_W) = A_N\psi_N + A_S\psi_S + A_E\psi_E + A_W\psi_W + (S_\psi)_P \text{ vol} \tag{28}$$

where $A_E = D_{x_+} - C_{x_+}$, $A_W = D_{x_-} + C_{x_-}$, etc., and, for high cell Reynolds numbers, these coefficients are modified according to the hybrid scheme of Gosman *et al.* [18].

If the pressure is known, then (28), written for each variable at each grid node, yields a closed set of algebraic equations, but there is no guarantee that the resultant velocity field would satisfy the continuity relation. The two problems of determining the pressure and satisfying continuity are overcome by adjusting the pressure field so as to satisfy continuity. The details of this procedure are given elsewhere (Gosman and Pun [1]) but it should be noted that it requires a specific juxtaposition of the velocity and pressure nodes (see Fig. 4). The pressure and other scalars are stored at the location (x_i^1, x_j^2) while the corresponding U- and V-velocities are stores at $[1/2(x_i^1 + x_{i-1}^1), x_j^2]$ and $[x_i^1, 1/2(x_j^2 + x_{j-1}^2)]$, respectively. An advantage of this scheme is that, for scalar equations, the normal velocity is known at each face of the cell and, consequently, interpolation is avoided.

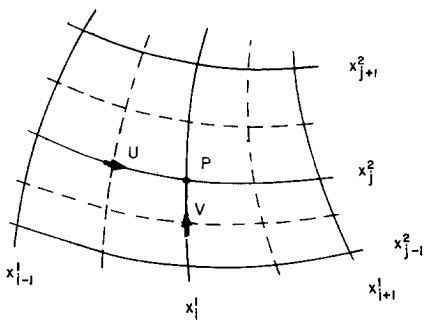

FIG. 4. Juxtaposition of grid nodes.

Attention is now focused on the computational problems posed by the curvilinear grid: the cell-face areas, the distance between grid nodes and the cell volumes, cannot be calculated from x^1 and x^2 as would be the case in Cartesian coordinates but require evaluation from, or storage as, two-dimensional quantities. If these quantities were stored it would involve five storage locations for each cell and, as there are three separate grids, this results in 15 storage locations per triad of nodes: thus, for a 30×30 grid, 13,500 storage locations would be required. Although this is a large storage requirement, the geometry is calculated only once, whereas another possibility would be to store only the Cartesian coordinates of the grid line intersections and to calculate the geometric parameters each time they are required. This scheme requires only eight storage locations per triad of nodes but evaluating lengths through

Pythagoras' theorem is computationally expensive. The method adopted is a compromise requiring twelve storage locations and a minimum of arithmetic: it is based on the "double" grid formed by the intersection of all the lines on Fig. 4, both full and broken. The distance between each intersection is stored in the manner shown in Fig. 5 as are the volumes of each of the four "quarter-cells" surrounding the pressure node. Thus, the cell-face areas appropriate to any node (U, V, or p) are given by the sum of two of these lengths and the cell volumes are given by the sum of four quarter-cell volumes. A further saving could be accomplished by storing the volume of the complete U, V, and p cells but, it will be shown below, a knowledge of the four quarter-cell volumes proves useful in evaluating the source terms.

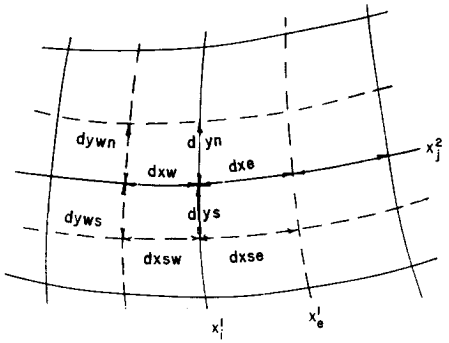

FIG. 5. Finite-difference grid representation.

The essential components of the finite-difference formulation have now been presented and, for details of the solution procedure, the reader is referred to Gosman and Pun [1]: there are, however, two further points worthy of mention. The first relates to the finite-difference approximation for the convective term (25) which, through the relation

$$\psi|_{x_+^1} \approx \tfrac{1}{2}(\psi_P + \psi_E), \tag{29}$$

implicitly assumes an evenly disposed grid. For a scalar equation on a Cartesian grid the cell boundaries do lie halfway between grid nodes and so (29) is appropriate: for the velocity equations this is not necessarily the case and so linear interpolation is employed. General orthogonal grids add a further complication because linearity in the coordinate system does not reflect linearity in physical space; that is, referring to Fig. 5, although $x_e^1 = 1/2(x_i^1 + x_{i+1}^1)$, it does not follow that $dxe_{i,j} = dxw_{i+1,j}$. Consequently, in refining the procedure, it would be appropriate to replace (25) by an approximation based on the assumption of linearity in physical space.

The second point, which has equal bearing on Cartesian procedures, relates to the evaluation of the production of turbulent kinetic energy, P. The method adopted here provides a more accurate volume integral than does (27) and treats the linkage between stress and strain consistently: the same finite-difference approximations for stress and strain are used in this context as are used in the momentum equations.

In Appendix II, P is expressed as the sum of the squared normal strains plus the square of the shear strain and, for variable density flows, terms involving the divergence of the velocity. Both the normal strains and the divergence of velocity are readily evaluated at the pressure node but the shear strains are known at each corner of the cell. Thus, the volume integral of the production of kinetic energy is evaluated from the normal strain and divergence terms at the pressure node multiplied by the cell volume plus the sum of the shear strain terms at the cell corners multiplied by the appropriate quarter-cell volume. The cell corners were also found to be the most convenient locations at which to store the coordinate variation terms $H_1(2)$ and $H_2(1)$.

In summary, it has been shown that the similarity of the transport equations expressed in general orthogonal coordinates and in Cartesian coordinates allows Gosman and Pun's [1] procedure to be used with the following modifications:

(a) The incorporation of the additional source terms given in Table I.

(b) Storing cell-face areas and cell volumes as two-dimensional quantities (which, along with $H_1(2)$ and $H_2(1)$, increases the storage requirement by 14 locations per grid node).

(c) Incorporating linear interpolation in physical space.

5. Grid-Generation Procedure

A procedure is described which determines the Cartesian coordinates, $\bar{x}$, of the nodes of an orthogonal grid. For a given specification of grid boundary, for example, the duct shape shown on Fig. 1b, and for the number and disposition of coordinate lines selected in each direction, the locations of the coordinate line intersections are determined. Consequently, by approximating the coordinate line between two nodes as a straight line, the grid distances shown on Fig. 5 can be calculated.

Referring to Fig. 2, the condition of orthogonality leads to the following relations,

$$\begin{aligned} d\bar{x}^1 &= h_1\, dx^1 \cos\theta + h_2\, dx^2 \sin\theta, \\ d\bar{x}^2 &= -h_1\, dx^1 \sin\theta + h_2\, dx^2 \cos\theta, \end{aligned} \tag{30}$$

from which it follows,

$$\frac{\partial \bar{x}^1}{\partial x^1} = \frac{h_2}{h_1}\frac{\partial \bar{x}^2}{\partial x^2}; \qquad \frac{\partial \bar{x}^2}{\partial x^1} = -\frac{h_2}{h_1}\frac{\partial \bar{x}^1}{\partial x^2} \tag{31}$$

and consequently

$$\nabla^2 \bar{x}^1 = 0, \qquad \nabla^2 \bar{x}^2 = 0 \tag{32}$$

where

$$\nabla^2 = \nabla(i)\frac{\partial}{\partial x(i)} = |\, h\,|^{-1}\left\{\frac{\partial}{\partial x^1}\frac{h_1}{h_2}\frac{\partial}{\partial x^1} + \frac{\partial}{\partial x^2}\frac{h_2}{h_1}\frac{\partial}{\partial x^2}\right\}. \tag{33}$$

Thus, the Cartesian coordinates of the orthogonal grid, $\bar{x}^1$ and $\bar{x}^2$, are seen to satisfy Laplace's equation but, in this instance, its solution is not uniquely determined by the boundary conditions since the scale factors in the Laplacian are functions of the solution: that is, some function of the scale factors must be prescribed throughout the solution domain in order that the equations be determinate. This is most readily achieved by prescribing a constant value to the ratio $a \equiv h_2/h_1$ everywhere which allows Eqs. (32) to be rewritten as,

$$\frac{\partial^2 \bar{x}^1}{\partial x^{1\,2}} + a^2 \frac{\partial^2 \bar{x}^1}{\partial x^{2\,2}} = 0, \qquad \frac{\partial^2 \bar{x}^2}{\partial x^{1\,2}} + a^2 \frac{\partial^2 \bar{x}^2}{\partial x^{2\,2}} = 0. \tag{34}$$

In order to determine the boundary conditions appropriate to (34), consider the general situation illustrated in Fig. 6 in which the domain bounded by the lines

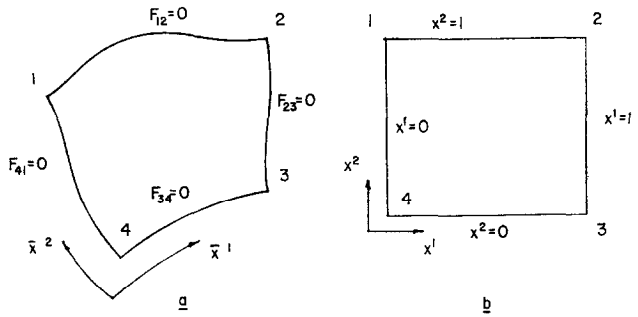

FIG. 6. Solution domain: (a) in Cartesian space; (b) in orthogonal space.

$F_{12} = 0$, $F_{23} = 0$, $F_{34} = 0$, and $F_{41} = 0$ is to be represented in the orthogonal x^1, x^2-space. The solution of (34) in the x^1, x^2-space requires the specification of eight boundary conditions (two on each side) and the determination of the constant a which is unique for a given set of boundary conditions in each space. One boundary condition on each side is provided by the loci of the boundary (i.e., $F_{12} = 0$, etc.) while another is deduced from either of Eq. (31) by

$$\bar{x}^1 = a \int \frac{\partial \bar{x}^2}{\partial x^2}\, dx^1 \qquad \text{or} \qquad \bar{x}^2 = -a \int \frac{\partial \bar{x}^1}{\partial x^2}\, dx^1 \tag{35}$$

for the sides 12 and 34 or, for the sides 23 and 41,

$$\bar{x}^2 = a^{-1} \int \frac{\partial \bar{x}^1}{\partial x^1}\, dx^2 \qquad \text{or} \qquad \bar{x}^1 = -a^{-1} \int \frac{\partial \bar{x}^2}{\partial x^1}\, dx^2. \tag{36}$$

Further, since $\bar{x}^1$ and $\bar{x}^2$ are known at each corner, a can be determined from any of the above relations.

An appreciation of the interrelation of the boundary conditions may be gained by examining their application to the side 12, for example: as illustrated on Fig. 6, the

shape of the domain may be such that the function $F_{12}(\bar{x}^1, \bar{x}^2)$ can be made explicit for $\bar{x}^2$, i.e.,

$$\bar{x}^2 = F_{12}(\bar{x}^1), \tag{37}$$

and so this relation, together with the first of Eqs. (35),

$$\bar{x}^1 = a \int \partial \bar{x}^2 / \partial x^2 \, dx^1, \tag{38}$$

form sufficient boundary conditions. In general, however, an explicit expression for $\bar{x}^2$ in terms of $\bar{x}^1$ (or vice versa) may not exist over the whole length of one side since $\bar{x}^2$ need not be a single-valued function of $\bar{x}^1$. Consequently, the implicit solution of $F_{12} = 0$ can have more than one root, introducing an ambiguity which can be avoided (or at least minimized) by adopting the following procedure. In regions where $\partial F_{12}/\partial \bar{x}^1 < \partial F_{12}/\partial \bar{x}^2$, (38) is employed to determine $\bar{x}^1$, and $\bar{x}^2$ is deduced from

$$F_{12}(\bar{x}^1, \bar{x}^2) = 0. \tag{39}$$

In regions where $\partial F_{12}/\partial \bar{x}^1 > \partial F_{12}/\partial \bar{x}^2$, $\bar{x}^2$ is determined from

$$\bar{x}^2 = -a \int \partial \bar{x}^1 / \partial x^2 \, dx^1 \tag{40}$$

and $\bar{x}^1$ is deduced from F_{12}. That is, the boundary conditions are applied piecewise in such a way as to minimize any ambiguity by solving (39) for whichever of $\bar{x}^1$ or $\bar{x}^2$ is least likely to be double valued.

Equations (34) are solved by a straightforward finite-difference method involving a five-point scheme. The finite-difference equations are solved iteratively, line by line and after each iteration the boundary conditions and the value of a are updated. No relaxation was used in solving the finite-difference equations but an underrelaxation factor of 0.1 was applied to the updating of a: this does not necessarily represent an optimum value but it results in satisfactory convergence rates without affecting stability. Figure 7 shows an example of the grids produced by this method where alternate grids lines have been drawn to correspond to the basic grid used by the main procedure. It may be seen that uneven spacing has been used in order to concentrate nodes into regions where large variations in flow properties are expected.

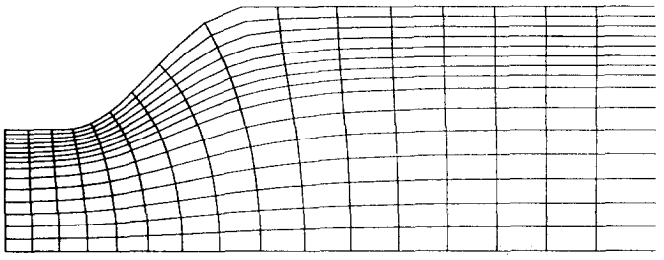

FIG. 7. Example of orthogonal grids generated.

6. Results and Discussion

A variety of simple flows were calculated in order to test the procedure. First, various aspects of the scheme were tested by calculating laminar flows with analytic solutions in which the flow is aligned with grid lines. For these cases the only inaccuracy was that caused by round-off error: the calculation of plane, linear shear, in Cartesian coordinates confirmed the correct treatment of the velocity-gradient terms and solid body rotation, calculated in polar–cylindrical coordinates, verified the treatment of pressure gradients. Linear, radial shear again calculated in polar–cylindrical coordinates was used to test the implementation of the additional terms due to coordinate curvature.

In order to test the treatment of the convective terms, a flow not aligned with the coordinate system was chosen. Plane, quadratic shear was calculated in polar

(in the usual notation) on an 11×11 grid and the velocity profile for $\theta = 0.55$ is compared with the analytic solution on Fig. 8. The maximum departure of the calculated value is 2.4% indicating that the scheme is prone to error due to false diffusion but not more than any other of the same genre.

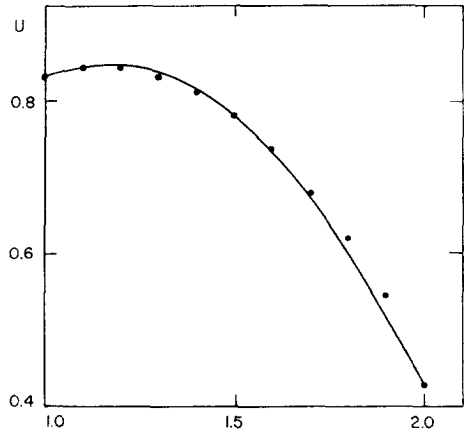

FIG. 8. U_1 against r; $\theta = 0.55$. Comparison of calculations with analytic result.

To test the procedure for turbulent flows is more difficult since analytic solutions are not available. However, the turbulent recirculating flow over a backward facing step was calculated in Cartesian coordinates and compared with similar calculations performed with the original, Cartesian-coordinate, version of the algorithm: the agreement between the results was within round-off error. This, and the other tests mentioned, confirms that the level of accuracy of the procedure is the same as that of the Cartesian version from which it was developed but to establish this level under a variety of different flow conditions would be a separate, though valuable, exercise.

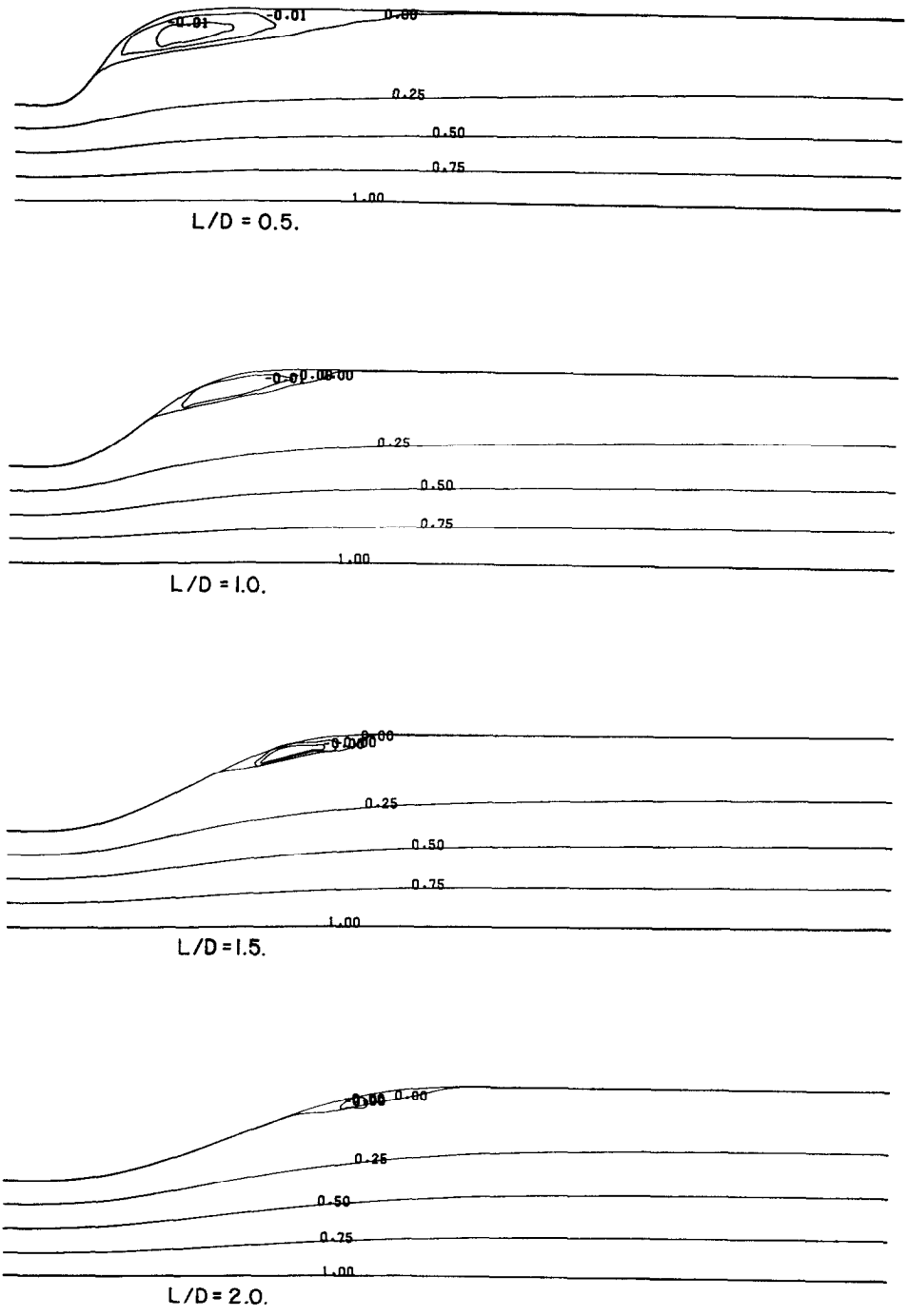

FIG. 9. Contours of stream function in diffusers of various expansion rates.

The combined grid-generation and flow calculation procedures were used to calculate flow properties in a symmetric duct resembling a diffuser: the initial width of the duct, D, was doubled by a sinusoidal curve of length L. Contours of stream function (defined to be zero at the wall and unity at the center line) are shown on Fig. 9 for values of L/D between 0.5 and 2.0. The calculations, performed on 20×16 grids such as that shown on Fig. 7, clearly show that the intensity and extent of the separated flow decreases with increasing values of L/D. Further results, and a discussion of their physical significance are reported elsewhere [19], and those shown on Fig. 9 are solely intended to demonstrate the capability of the procedure. The time and storage requirements of the Fortran computer program are 0.004 sec/grid node/iteration (CDC 6600) and 11,000 words + 31 words/grid node. For the 20×16 grids mentioned above, 150 iterations were required for convergence leading to 190 sec of computation using 21,000 words of memory. The time requirement is comensurate with the original procedure but the storage requirement, though not excessive, is increased by 14 words/grid node.

In conclusion, a finite-difference procedure has been developed to calculate the mean properties of turbulent recirculating flows in general orthogonal coordinates. With only a small penalty of computer storage, this allows flows bounded by curved surfaces to be calculated more easily, efficiently, and accurately than is possible in Cartesian coordinates. A novel method of transforming quantities into general orthogonal coordinates has been presented which facilitates the incorporation of a variety of transport equations into the scheme. In addition, a grid-generation procedure, based on the solution of Laplace's equation by finite-difference means, has been developed. The procedure has been tested and sample calculations of turbulent recirculating flows have been performed.

APPENDIX I

A four-step procedure is presented for transforming equations written in Cartesian tensors into general orthogonal coordinates; and, the transformation relations established here allow equations to be transformed in a single step. The momentum equation, (2), is used as an example.

Step 1. Write the equation in general tensor notation:

$$\partial/\partial t\, \rho U_j + (\rho U^i U_j)_{,i} = -p_{,j} - \tau^i_{j,i}\,.$$

Step 2. Define the physical-component derivative as

$$A(ij \cdots lm); n \equiv \frac{h_i h_j \cdots}{h_l h_m \cdots h_n} A^{ij\cdots}_{\cdots lm,n}$$

and multiply or divide the general tensor equation by the appropriate scale factors in order to obtain the equation in physical component form:

$$[\partial \rho U(j)/\partial t] + [\rho U(i)\, U(j) + \tau(ij)]; \leftarrow i = -p;\ j.$$

Step 3. Expand the equation in terms of known quantities (e.g., h_i) and operators (e.g., $\partial/\partial x(i)$). This step will prove to be no more complicated than the previous two, but some delay is required here in order to establish the relationship between the physical component derivative and known quantities.

The particular form of the metric tensor in orthogonal coordinates, i.e., $g_{ij} = h_i^2 \delta_{ij}$, allows the physical-component derivative to be related to the covariant derivative of a covariant tensor:

$$\begin{aligned}\frac{h_i h_j \cdots}{h_l h_m \cdots h_n} A^{ij\cdots}{}_{\cdots lm,n} &= \frac{h_i h_j \cdots}{h_l h_m \cdots h_n} g^{pi} g^{qj} \cdots A_{pq\cdots lm\cdots,n} \\ &= \frac{1}{h_i h_j \cdots h_l h_m \cdots h_n} A_{ij\cdots lm,n} \\ &= A(ij \cdots lm); n.\end{aligned}$$

And, expanding the left-hand side gives

$$A(ij \cdots lm); n = \frac{1}{h_i h_j \cdots h_l h_m \cdots h_n} \left[\frac{\partial A_{ij\cdots lm}}{\partial x^n} - A_{sj\cdots lm} \begin{Bmatrix} s \\ i \quad n \end{Bmatrix} - \cdots A_{ij\cdots ls} \begin{Bmatrix} s \\ m \quad n \end{Bmatrix} \right]$$

where the Christoffel symbols are given by

$$\begin{Bmatrix} s \\ p \quad q \end{Bmatrix} = g^{sr}(pq, r)$$

and

$$(pq, r) = \frac{1}{2}\left(\frac{\partial g_{pr}}{\partial x^q} + \frac{\partial g_{qr}}{\partial x^p} - \frac{\partial g_{pq}}{\partial x^r} \right).$$

Substituting the particular form of the metric tensor into these relations leads to

$$\frac{1}{h_i h_j \cdots h_l h_m \cdots h_n} A_{sj\cdots lm} \begin{Bmatrix} s \\ i \quad n \end{Bmatrix} = A(ij \cdots lm)\, H_s(n) + A(sj \cdots lm) \begin{pmatrix} s \\ i \quad n \end{pmatrix}$$

where

$$H_i(j) \equiv (1/h_i h_j)\, \partial h_i / \partial x^j$$

and

$$\begin{pmatrix} s \\ i \quad n \end{pmatrix} = H_s(i)\, \delta_{sn} - H_i(s)\, \delta_{in}\,.$$

Thus, with the further relation,

$$\frac{\partial A(ij \cdots lm)}{\partial x(n)} = \frac{1}{h_i h_j \cdots h_l h_m h_n} \frac{\partial A_{ij\cdots lm}}{\partial x^n} - A(ij \cdots lm) \sum_{s=ij\cdots lm} H_s(n)$$

the physical-component derivative is given by,

$$A(ij \cdots lm); n = \frac{\partial A(ij \cdots lm)}{\partial x(n)} - A(sj \cdots lm)\begin{Bmatrix} s \\ i \quad n \end{Bmatrix} \cdots - A(ij \cdots ls)\begin{Bmatrix} s \\ m \quad n \end{Bmatrix}.$$

It may be seen that this expression is directly analogous to the covariant derivative of a covariant tensor and, consequently, $\{{}_i{}^s{}_n\}$ can be regarded as the physical-component Christoffel symbol.

In addition to the physical-component derivative, the divergence operator $\nabla(p)$ is defined so that Green's theorem can be applied;

$$\nabla(p) \equiv |h|^{-1} \partial/\partial x^p \, |h|/h_p .$$

It is readily shown that the physical component derivative and divergence are related by,

$$\nabla(i)\, A(ij \cdots lm) = A(ij \cdots lm); i + A(is \cdots lm)\begin{Bmatrix} s \\ j \quad i \end{Bmatrix} \cdots A(ij \cdots ls)\begin{Bmatrix} s \\ m \quad i \end{Bmatrix}.$$

Thus, the application of the third step to the momentum equation yields,

$$\frac{\partial \rho U(j)}{\partial t} + \nabla(i)[\rho U(i)\, U(j) + \tau(ij)] - [\rho U(i)\, U(s) + \tau(is)]\begin{Bmatrix} s \\ j \quad i \end{Bmatrix} = -\frac{\partial p}{\partial x(j)}.$$

Step 4. Expand the physical component Christoffel symbols;

$$\frac{\partial \rho U(j)}{\partial t} + \nabla(i)\,[\rho U(i)\, U(j) + \tau(ij)] = -\frac{\partial p}{\partial x(j)} + H_i(j)[\rho U(i)\, U(i) + \tau(ij)] - H_j(i)[\rho U(i)\, U(j) + \tau(ij)].$$

From this procedure it is evident that the following transformations exist between quantities $\bar{A}$ in a coordinate system $\bar{x}$ and the equivalent quantity, A, in the general orthogonal system x:

$$\bar{A}_{ij\ldots lm} \to A(ij \cdots lm),$$

$$\frac{\partial \bar{A}_{ij\ldots lm}}{\partial \bar{x}_n} \to \frac{\partial A(ij \cdots lm)}{\partial x(n)} - A(nj \cdots lm)\, H_n(i) + A(sj \cdots lm)\, H_i(s)\, \delta_{in} \cdots - A(ij \cdots ln)\, H_n(m) + A(ij \cdots ls)\, H_m(s)\, \delta_{mn},$$

$$\frac{\partial \bar{A}_{ij\ldots lm}}{\partial \bar{x}_i} \to \nabla(i)\, A(ij \cdots ln) - A(ii \cdots lm)\, H_i(j) + A(ji \cdots lm)\, H_j(i) \cdots - A(ij \cdots li)\, H_i(m) + A(mj \cdots li)\, H_m(i).$$

These transformations written for a scalar, a vector, and a second-order tensor are quoted in the text and allow the transport equations to be expressed in general orthogonal coordinates.

APPENDIX II

The transport equations in orthogonal coordinates, when expanded for two-dimensional, steady flows, can be expressed in the common form:

$$\nabla_x(\rho U\psi - \Gamma_x\,\partial\psi/\partial x) + \nabla_y(\rho V\psi - \Gamma_y\,\partial\psi/\partial y) = S_\psi$$

where,

$$dx(1) = dx, \qquad U(1) = U,$$
$$dx(2) = dy, \qquad U(2) = V,$$
$$\nabla_x = (1/h_2)\,\partial/\partial x\,h_2\,, \qquad \nabla_y = (1/h_1)\,\partial/\partial y\,h_1\,,$$

and the values of Γ_x, Γ_y, and S_ψ appropriate to each variable are given in Table I. $\psi = 1$ corresponds to the continuity equation and the diffusivities and source appropriate to the V-equation are obtained from the U-equation by commuting U and V, 1 and 2, and x and y. The effective viscosity formula, being a scalar function of scalars, is the same as in Cartesian tensors while the production of kinetic energy is given by

$$P = \mu_{\text{eff}}\left\{2\left[\frac{\partial U}{\partial x} + VH_1(2)\right]^2 + 2\left[\frac{\partial V}{\partial y} + UH_2(1)\right]^2 + \left[\frac{\partial U}{\partial y} + \frac{\partial V}{\partial x} - UH_1(2) - VH_2(1)\right]^2\right\} - \frac{2}{3}[\rho k + \mu_{\text{eff}}(\nabla_x U + \nabla_y V)](\nabla_x U + \nabla_y V).$$

ACKNOWLEDGMENTS

The author is pleased to acknowledge helpful discussions with colleagues at Imperial College and is particularly indebted to Dr. Tuncer Cebeci for his help and encouragement.

REFERENCES

1. A. D. GOSMAN AND W. M. PUN, "Calculation of Recirculating Flows," Imperial College, Dept. of Mech. Engng. Report, HTS/73/2, 1973.
2. S. B. POPE AND J. H. WHITELAW, *J. Fluid Mech.* **73** (1976), 9.
3. E. E. KHALIL, D. B. SPALDING, AND J. H. WHITELAW, *Int. J. Heat Mass Transfer* **18** (1975), 775.
4. S. G. RUBIN, NASA SP-378, 1975 (collected work).
5. C. W. HIRT, A. A. AMSDEN, AND J. L. COOK, *J. Computational Phys.* **14** (1974), 227.
6. W. E. PRACHT, *J. Computational Phys.* **17** (1975), 132.
7. B. E. LAUNDER AND D. B. SPALDING, "Mathematical Models of Turbulence," Academic Press, London, 1972.

8. S. B. POPE, *Combust. Flame* **29** (1977), 235.
9. W. D. BARFIELD, *J. Computational Phys.* **5** (1970), 23.
10. A. A. AMSDEN AND C. W. HIRST, *J. Computational Phys.* **11** (1973), 348.
11. J. F. THOMPSON, F. C. THAMES, AND C. W. MASTIN, *J. Computational Phys.* **15** (1974), 299.
12. B. E. LAUNDER, "Numerical Computation of Convective Heat Transfer in Complex Turbulent Flows," Ph.D. Thesis, University of London, 1971; also, W. P. Jones and B. E. Launder, *Int. J. Heat Mass Transfer* **15** (1972), 301.
13. P. Y. CHOU, *Quart. Appl. Math.* **3** (1945), 38.
14. F. H. HARLOW AND P. I. NAKAYAMA, *Phys. Fluids* **10** (1967), 323.
15. S. B. POPE, *J. Fluid Mech.* **72** (1975), 337.
16. S. B. POPE, "The Limits of Applicability of Turbulent Scale Equations," Imperial College, Dept. of Mech. Engng, Report, CHT/76/7, 1976.
17. S. B. POPE, "The Calculation of the Flow Behind Bluff Bodies with and without Combustion," Ph.D. Thesis, University of London, 1976.
18. A. D. GOSMAN, W. M. PUN, A. K. RUNCHAL, D. B. SPALDING, AND M. WOLFSHTEIN, "Heat and Mass Transfer in Recirculating Flows," Academic Press, London, 1968.
19. S. B. POPE, "The Calculation of Separated Boundary Layers," Symposium on Turbulent Shear Flows, Pennsylvania State University, April 1977.